J|A|C|S
ARTICLES
Published on Web 01/14/2006

A Threaded Loop Conformation Adopted by a Family of Peptoid Nonamers

Kai Huang,[†,‡] Cindy W. Wu,[§] Tracy J. Sanborn,[§] James A. Patch,[§] Kent Kirshenbaum,[¶] Ronald N. Zuckermann,[#] Annelise E. Barron,*[,§] and Ishwar Radhakrishnan*[,†]

Contribution from the Department of Biochemistry, Molecular Biology and Cell Biology, Northwestern University, Evanston, Illinois 60208, Structural Biology NMR Facility, Northwestern University, Evanston, Illinois 60208, Departments of Chemical and Biological Engineering and Chemistry, Northwestern University, Evanston, Illinois 60208, Department of Chemistry, New York University, New York, New York 10003, and Chiron Technologies, Chiron Corporation, Emeryville, California 94608

Received November 9, 2005; E-mail: a-barron@northwestern.edu; i-radhakrishnan@northwestern.edu

Abstract: Non-natural polymers with well-defined three-dimensional folds offer considerable potential for engineering novel functions that are outside the scope of biological polymers. Here we describe a family of N-substituted glycine or "peptoid" nonamers that folds into an unusual "threaded loop" structure of exceptional thermal stability and conformational homogeneity in acetonitrile. The structure is chain-length-specific and relies on bulky, chiral side chains and chain-terminating functional groups for stability. Notable elements of the structure include the engagement of the positively charged amino terminus by carbonyl groups of the backbone through hydrogen bonding interactions and shielding of polar groups from and near-complete exposure of hydrophobic groups to solvent, in a manner resembling a folded polypeptide globular domain turned inside-out. The structure is stable in a variety of organic solvents but is readily denatured in any solvent/cosolvent milieu with hydrogen bonding potential. The structure could serve as a scaffold for the elaboration of novel functions and could be used to test methodologies for predicting solvent-dependent polymer folding.

Introduction

Form and function in biology are intimately related. Biological polymers, with their rich repertoire of accessible secondary and tertiary structures coupled with the ability to fold into unique, thermodynamically stable shapes, have inspired the design and development of non-natural polymers capable of performing novel functions.[1,2] An astonishing variety of non-natural scaffolds, termed "foldamers", including β-peptides,[3,4] γ-peptides,[5,6] oligomers of N-substituted glycines (peptoids),[7,8] phenylene ethynylenes,[9] and urea derivatives,[10] have been described that can mimic helical or sheet-like secondary structures found in polypeptides. Successful engineering of stably folded tertiary structures has been largely elusive, although steady progress toward supersecondary structures, such as helical bundles, is being made in the case of β-peptides and peptoids.[11−14] Here we describe the serendipitous discovery and subsequent characterization of a stable, discretely folded conformation adopted by a family of peptoid oligomers.

The fundamental building block of a polypeptoid has the properties of a glycine (a methylene group in the backbone) and a proline (substitution at the amide nitrogen), two amino acid residues endowed with contrasting degrees of conformational freedom at the backbone level in proteins. Previous experimental and theoretical studies have shown that increased bulkiness of the peptoid side chain can greatly limit the accessible conformational space of the backbone.[8,15,16] This property has been used gainfully to further bias the peptoid

[†] Department of Biochemistry, Molecular Biology and Cell Biology, Northwestern University.
[‡] Structural Biology NMR Facility, Northwestern University.
[§] Departments of Chemical and Biological Engineering and Chemistry, Northwestern University.
[¶] New York University.
[#] Chiron Corporation.

(1) Gellman, S. H. *Acc. Chem. Res.* **1998**, *31*, 173−180.
(2) Hill, D. J.; Mio, M. J.; Prince, R. B.; Hughes, T. S.; Moore, J. S. *Chem. Rev.* **2001**, *101*, 3893−4012.
(3) Seebach, D.; Matthews, J. L. *Chem. Commun.* **1997**, 2015−2022.
(4) Cheng, R. P.; Gellman, S. H.; DeGrado, W. F. *Chem. Rev.* **2001**, *101*, 3219−3232.
(5) Seebach, D.; Brenner, M.; Rueping, M.; Jaun, B. *Chemistry* **2002**, *8*, 573−584.
(6) Woll, M. G.; Lai, J. R.; Guzei, I. A.; Taylor, S. J.; Smith, M. E.; Gellman, S. H. *J. Am. Chem. Soc.* **2001**, *123*, 11077−11078.
(7) Simon, R. J.; et al. *Proc. Natl. Acad. Sci. U.S.A.* **1992**, *89*, 9367−9371.
(8) Kirshenbaum, K.; Barron, A. E.; Goldsmith, R. A.; Armand, P.; Bradley, E. K.; Truong, K. T.; Dill, K. A.; Cohen, F. E.; Zuckermann, R. N. *Proc. Natl. Acad. Sci. U.S.A.* **1998**, *95*, 4303−4308.
(9) Hill, D. J.; Moore, J. S. *Proc. Natl. Acad. Sci. U.S.A.* **2002**, *99*, 5053−5057.
(10) Semetey, V.; Rognan, D.; Hemmerlin, C.; Graff, R., Briand, J.-P.; Marraud, M.; Guichard, G. *Angew. Chem., Int. Ed.* **2002**, *41*, 1893−1895.
(11) Raguse, T. L.; Lai, J. R.; LePlae, P. R.; Gellman, S. H. *Org. Lett.* **2001**, *3*, 3963−3966.
(12) Bruckner, A. M.; Chakraborty, P.; Gellman, S. H.; Diederichsen, U. *Angew. Chem., Int. Ed.* **2003**, *42*, 4395−4399.
(13) Burkoth, T. S.; Beausoleil, E.; Kaur, S.; Tang, D.; Cohen, F. E.; Zuckermann, R. N. *Chem. Biol.* **2002**, *9*, 647−654.
(14) Lee, B. C.; Zuckermann, R. N.; Dill, K. A. *J. Am. Chem. Soc.* **2005**, *127*, 10999−11009.

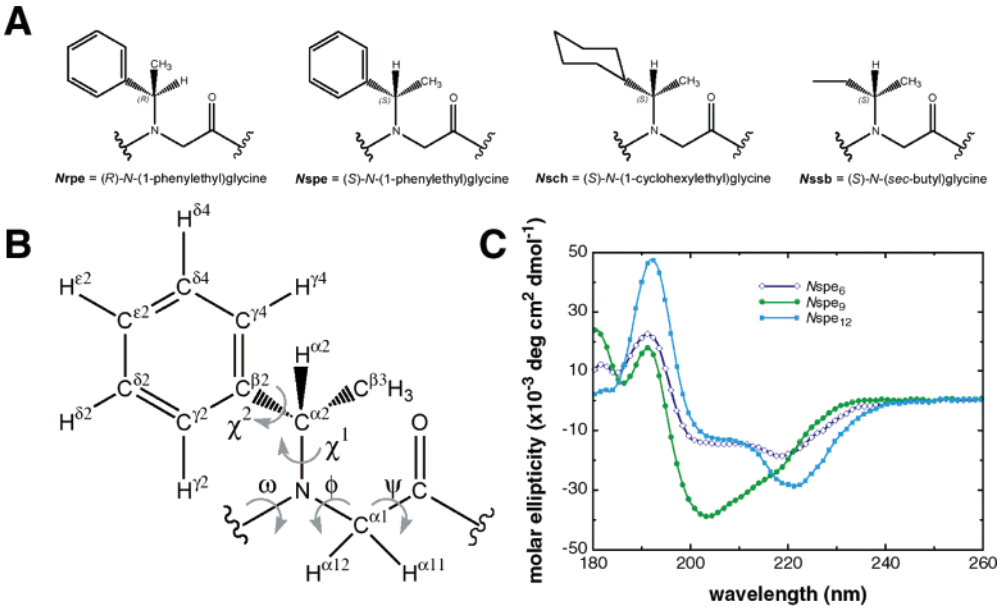

Figure 1. Peptoid designations and circular dichroism spectra. (A) Chemical structures of peptoid residues used in this study and their respective designations. (B) Nomenclature of peptoid atoms and dihedral angles following IUPAC conventions for *N*spe. (C) CD spectra of *N*spe oligomers of varying chain lengths recorded in neat acetonitrile at 25 °C. Peptoid concentration was ~60 μM. The distinctive banding pattern in the *N*spe$_9$ spectrum is readily apparent.

backbone toward polyproline type I (PPI) helical conformations through the introduction of a chiral center in the side chains.[17−20] Furthermore, by choosing the appropriate enantiomer, the overall handedness of the helix can be readily and predictably controlled.

Helical conformations for peptoids, unlike polypeptides, can be readily facilitated in a variety of solvents, including organic solvents such as methanol and acetonitrile. This is attributed to the contrasting mechanisms through which backbone conformations are populated in these polymers with steric and electronic factors playing dominant roles. The repertoire of secondary structures accessible to peptoids appears to be somewhat limited as only helical conformations have been described thus far, although the rules for engineering stable helices are now better understood.[17−20] An apt demonstration of this capability was provided by the successful mimicry of the amphipathic helical character as well as the biophysical functions of the lung surfactant proteins B (SP-B) and C (SP-C) by engineered peptoid oligomers ranging from 17 to 22 residues in length.[21,22] Unlike β-peptide and urea-based foldamers, the peptoid backbone is almost completely devoid of hydrogen bonding donors, which may be an important factor precluding the formation of β-hairpin/sheet-type secondary structures commonly found in polypeptides. Novel peptoid "folding units" are of considerable interest, and here we describe such a conformation that has the potential for further structural and functional elaboration.

Results and Discussion

Circular Dichroism Studies of *N*rpe and *N*spe Peptoids. Our previous studies aimed at clarifying the relationship between peptoid chain length and helicity in acetonitrile solvent revealed an unusual, nonhelical CD spectrum for the 9-residue homooligomer {*N*-(*R*)-(1-phenylethyl)glycine}$_9$, or *N*rpe$_9$.[17] *N*spe$_9$, which is the enantiomer of *N*rpe$_9$, exhibits a mirror image spectrum characterized by a minimum and a maximum of positive ellipticity at 187 and 192 nm, respectively, as well as a single, broad minimum of negative ellipticity at 203 nm (Supporting Information Figure S1). Intriguingly, the nonhelical spectrum appears to be unique to nonamer peptoids since other *N*spe homooligomers ranging between 6 and 15 residues in length displayed characteristic helical spectra with a maximum of negative ellipticity at 192 nm and minima of positive ellipticity at about 202 and 220 nm (Figure 1; a monomer-by-monomer evolution of *N*rpe$_n$ peptoid (n = 5−20) CD spectra is described in ref 18). Moreover, the *N*spe$_9$ spectrum remains essentially unchanged over a wide range of peptoid concentrations (1 μM to 1.5 mM; data not shown), implying that the peptoid does not self-associate to form a multimer.

NMR Spectroscopic Studies of *N*spe$_9$. Solution NMR studies were undertaken to gain insights into the unusual structure adopted by *N*spe$_9$ in acetonitrile. Notwithstanding the homopolymeric nature of the *N*spe$_9$ sequence, the ^{1}H−^{13}C HSQC spectrum was remarkably well dispersed (Figure 2), indicative of a nonrepetitive, folded conformation. Another hallmark of the spectrum was the presence of only a single set of resonances, implying exceptional conformational purity. These features are in marked contrast to those reported previously for peptoid oligomers that populate PPI conformations.[16,18] Furthermore, the spectrum was largely unchanged over a wide range of temperatures spanning from 25 to 65 °C, implying

(15) Armand, P.; Kirshenbaum, K.; Falicov, A.; Dunbrack, R. L., Jr.; Dill, K. A.; Zuckermann, R. N.; Cohen, F. E. *Fold. Des.* **1997**, *2*, 369−375.
(16) Armand, P.; Kirshenbaum, K.; Goldsmith, R. A.; Farr-Jones, S.; Barron, A. E.; Truong, K. T.; Dill, K. A.; Mierke, D. F.; Cohen, F. E.; Zuckermann, R. N.; Bradley, E. K. *Proc. Natl. Acad. Sci. U.S.A.* **1998**, *95*, 4309−4314.
(17) Wu, C. W.; Sanborn, T. J.; Zuckermann, R. N.; Barron, A. E. *J. Am. Chem. Soc.* **2001**, *123*, 2958−2963.
(18) Wu, C. W.; Sanborn, T. J.; Huang, K.; Zuckermann, R. N.; Barron, A. E. *J. Am. Chem. Soc.* **2001**, *123*, 6778−6784.
(19) Wu, C. W.; Kirshenbaum, K.; Sanborn, T. J.; Patch, J. A.; Huang, K.; Dill, K. A.; Zuckermann, R. N.; Barron, A. E. *J. Am. Chem. Soc.* **2003**, *125*, 13525−13530.
(20) Sanborn, T. J.; Wu, C. W.; Zuckermann, R. N.; Barron, A. E. *Biopolymers* **2002**, *63*, 12−20.
(21) Wu, C. W.; Seurynck, S. L.; Lee, K. Y.; Barron, A. E. *Chem. Biol.* **2003**, *10*, 1057−1063.
(22) Seurynck, S. L.; Patch, J. A.; Barron, A. E. *Chem. Biol.* **2005**, *12*, 77−88.

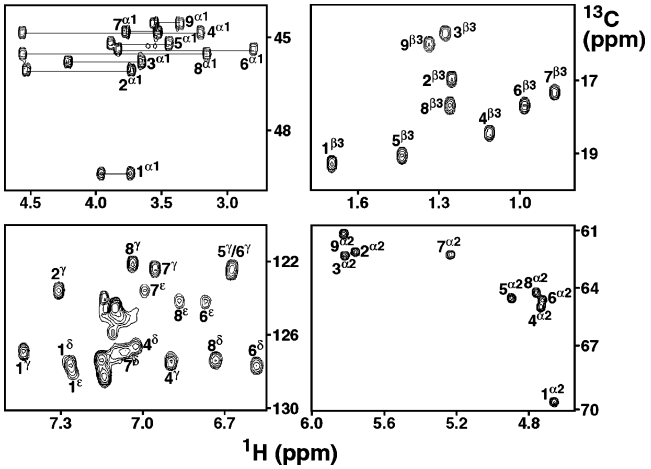

Figure 2. A discrete, folded conformation for *N*spe$_9$ revealed by solution NMR. Expanded plots of a ^{1}H−^{13}C HSQC spectrum recorded at natural ^{13}C abundance in neat acetonitrile at 25 °C. The panels (clockwise from top left) depict main chain methylene, side chain methyl, side chain methine, and aromatic correlations. Unambiguous, sequence-specific assignments are indicated. Notwithstanding the homopolymeric nature of the peptoid sequence, the spectrum is characterized by excellent chemical shift dispersion and a single set of correlations.

unusual thermal stability. To characterize the features of the novel conformation, we sought to assign the resonances in a sequence-specific manner. We employed an *N*spe$_9$ sample uniformly enriched in ^{13}C at the backbone carbon positions and adopted a through-bond correlation approach widely used for proteins for sequence-specific peptoid resonance assignments (Supporting Information Figure S2).[23,24] All aliphatic proton and carbon resonances were assigned in this manner, while most, except four, aromatic protons and carbons were unambiguously assigned as well.

The covalent attachment of substituents to the backbone amide nitrogen in peptoids, not unlike prolines in naturally occurring proteins, may dispose the peptoid bond (analogous to the peptide bond in polypeptides) to adopt either the *cis* or *trans* conformation. The two conformations give rise to distinct ^{1}H−^{1}H nuclear Overhauser effects (NOEs) that permit ready identification of the conformation of the ω torsion angle. The *cis* conformation is predicted to give rise to sequential NOEs involving main chain H$^{\alpha 1}$ protons, while the *trans* conformation is expected to result in sequential NOEs involving main chain H$^{\alpha 1}$ and side chain H$^{\alpha 2}$ protons. A similar pattern of NOEs is commonly used to discriminate between the two conformations in proline−proline dipeptide steps in proteins.[25] These criteria unambiguously established a *cis* conformation for peptoid bonds linking residues **1**−**2**, **2**−**3**, **6**−**7**, and **8**−**9**, and a *trans* conformation for those linking residues **3**−**4**, **4**−**5**, **5**−**6**, and **7**−**8** (Supporting Information Figure S3). The side chain ^{1}H$^{\alpha 2}$ and ^{13}C$^{\alpha 2}$ chemical shifts also appear to be correlated with the ω torsion angle. The chemical shifts of residues **2**, **3**, **7**, and **9** and residues **4**, **5**, **6**, and **8** fall into two distinct clusters (Figure 2). The former with downfield ^{1}H$^{\alpha 2}$ and upfield ^{13}C$^{\alpha 2}$ chemical shifts is correlated with the *cis* ω torsion angle, while the latter cluster with relatively upfield ^{1}H$^{\alpha 2}$ and downfield ^{13}C$^{\alpha 2}$ chemical shifts is correlated with the *trans* ω torsion angle. The magnetic anisotropy of the main chain carbonyl group is a likely origin for these differential effects.

Table 1. NMR Structure Determination Statistics for *N*spe$_9$

Restraint Statistics	
NOE-based distance restraints	167
unambiguous distance restraints	155
intraresidue	89
sequential ($\|i-j\|=1$)	24
medium-range ($1<\|i-j\|\le 4$)	17
long-range ($\|i-j\|>4$)	25
ambiguous distance restraints	12
torsion angle restraints	8
Structure Quality of the Ensemble	
restraint satisfaction	
RMS differences for distance restraints	0.009 ± 0.003 Å
RMS differences for dihedral angle restraints	1.061 ± 0.261°
deviations from ideal covalent geometry	
bond lengths	0.004 ± 0.000 Å
bond angles	0.889 ± 0.011°
impropers	0.650 ± 0.015°
Average Atomic RMSDs from the Average Structure	
all atoms	1.07 Å
all heavy atoms except C$^\gamma$, C$^\delta$, C$^\epsilon$ atoms	0.30 Å
backbone atoms (i.e., N, C$^{\alpha 1}$, C′)	0.16 Å

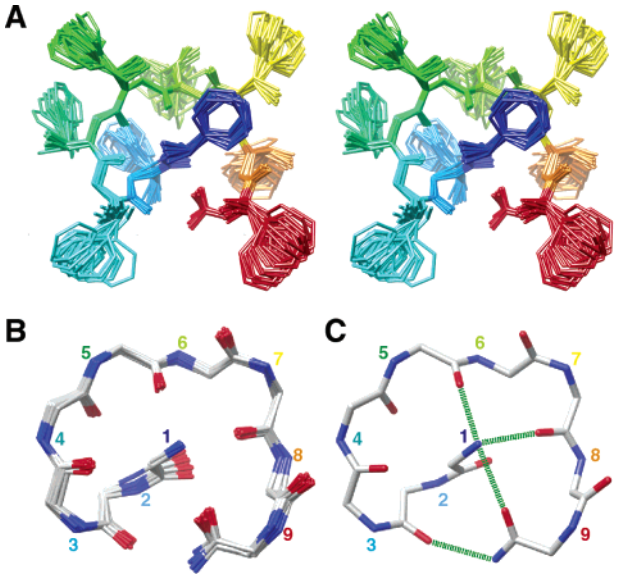

Figure 3. Solution structure of and stabilizing hydrogen bonding interactions in *N*spe$_9$. (A) Cross-eyed stereographic views of the ensemble of 20 NMR structures following a best-fit superposition of the backbone atoms. Residues from the N- to the C-terminus in the peptoid chain are color-ramped from blue to red following the rainbow pattern. (B) A view of the backbone atoms in the ensemble colored according to atom type (red, oxygen; blue, nitrogen; silver, carbon). The labels identify various residues in the chain. (C) The backbone of a representative structure from the ensemble. The dashed green lines denote hydrogen bonding interactions.

NMR Structure Determination of *N*spe$_9$. The exceptionally high quality of NMR spectra permitted a high-resolution structure determination of *N*spe$_9$. ^{1}H−^{1}H NOEs constituted the primary source of structural information, contributing an average of over 18 restraints per residue for these calculations. Because of the presumed atypical structure, a fully automated, iterative approach for NOE assignment and structure determination was adopted,[26] although all the assignments were checked manually

(23) Ferentz, A. E.; Wagner, G. Q. *Rev. Biophys.* **2000**, *33*, 29−65.
(24) Bradley, E. K.; Kerr, J. M.; Richter, L. S.; Figliozzi, G. M.; Goff, D. A.; Zuckermann, R. N.; Spellmeyer, D. C.; Blaney, J. M. *Mol. Diversity* **1997**, *3*, 1−15.
(25) Wüthrich, K. *NMR of Proteins and Nucleic Acids*, 1st ed.; Wiley-Interscience: New York, 1986; p 292.
(26) Linge, J. P.; Habeck, M.; Rieping, W.; Nilges, M. *Bioinformatics* **2003**, *19*, 315−316.

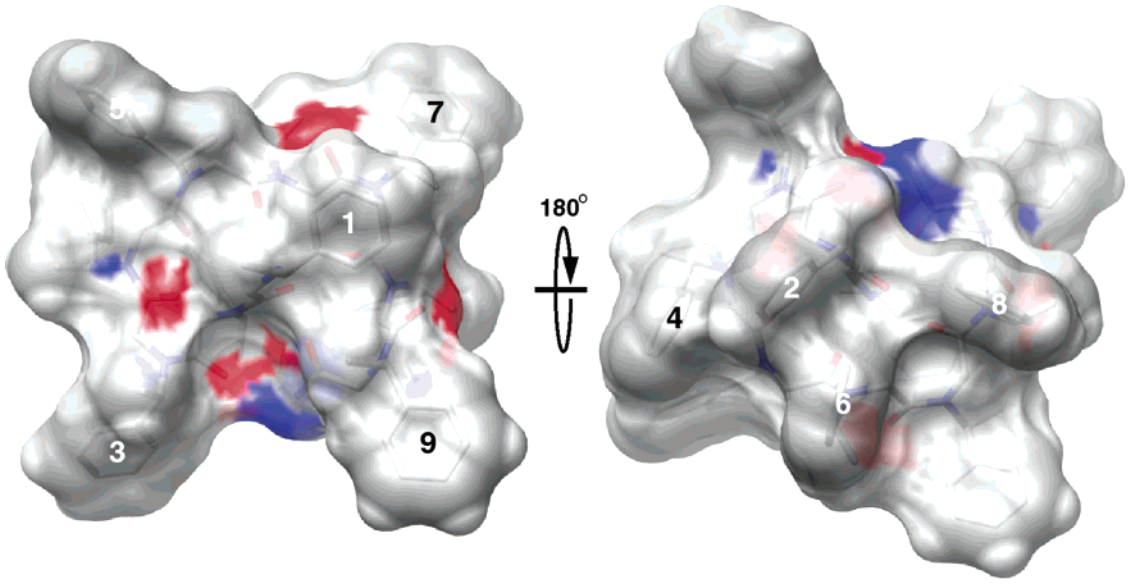

Figure 4. Near-complete shielding of the peptoid backbone by the aromatic side chains of *N*spe$_9$. Views of the molecular surface of *N*spe$_9$ rendered semi-transparently and color-coded according to atom type (red, oxygen; blue, nitrogen; silver, carbon). The view on the left is identical to those shown in Figure 3. The view on the right emphasizes packing interactions involving the aromatic side chains of residues **2**, **4**, and **6**.

during the intermediate stages and also upon conclusion of the refinement. The 20 structures that best satisfied the input experimental data possessed good stereochemistry (Table 1) and converged to the same fold with the backbone atoms in particular sampling a narrow range of conformations (Figure 3A and 3B).[27]

***N*spe$_9$ Structure Description.** The peptoid backbone of *N*spe$_9$ forms a rather elaborate, approximately planar loop-like structure (Figure 3C). The backbone atoms form a tightly packed "core" with the positively charged N-terminus serving as the organizing center. The protonated state of the N-terminus was confirmed by the detection of a pair of downfield-shifted resonances from the NH_2^+ group in the ^{1}H NMR spectrum. Like structured polypeptide loops, the conformation is stabilized by multiple hydrogen bonding interactions between the amino terminus and the carbonyl groups of residues **5**, **7**, and **9** (Figure 3C). The latter interaction brings the N- and C-termini together, thereby closing the loop through a noncovalent interaction. A complementary hydrogen bonding interaction between the capping amide group at the C-terminus and the backbone carbonyl group of residue **2** appears to play a cooperative role in loop closure. The involvement of chain terminal groups in these interactions explains why the conformation is specific to nonamer peptoids.

Compared to the peptoid backbone, the conformations of the apolar side chains are less well defined, with a progressive reduction in angular order for χ^2 compared to χ^1 (Figure 3A). The aromatic moieties of all nine residues are exposed to solvent. Interestingly, the aromatic groups of residues **3**, **5**, **7**, and **9** are symmetrically disposed radiating outward, but in the same plane as the backbone (Figure 4). The side chains of residues **2**, **4**, and **6** interact with each other through the aromatic moieties and form a protective sheath covering the backbone on one side of the planar surface. The entire side chain of residue **1** along with the side chain methyl groups of residues **3**, **5**, **7**, and **9** cover the other side of the surface (Figure 4). The peptoid backbone is thus effectively shielded from solvent while the side chains are exposed, resembling a protein globular domain turned inside-out. The unusual arrangement of the side chain of residue **1** together with the closed loop conformation for the backbone leads us to propose the term "threaded loop" to describe the overall peptoid conformation.

Table 2. Ensemble Averages for *N*spe$_9$ Main Chain and Side Chain Dihedral Angles (°)

residue	ϕ	ψ	ω	χ^1
1		−175.34 ± 4.35	−0.14 ± 2.06	
2	−68.40 ± 3.73	154.92 ± 4.37	0.15 ± 2.76	−114.89 ± 09.72
3	−69.92 ± 3.15	159.83 ± 4.31	−176.10 ± 0.90	−109.10 ± 05.21
4	76.08 ± 4.78	−177.68 ± 6.29	−177.10 ± 0.76	−130.34 ± 13.69
5	−72.85 ± 4.72	172.54 ± 6.04	−179.87 ± 2.27	−99.20 ± 09.86
6	−76.68 ± 6.30	−177.96 ± 4.38	−3.13 ± 0.50	−117.28 ± 18.09
7	−78.04 ± 3.57	−158.13 ± 6.59	177.83 ± 1.50	−87.58 ± 08.98
8	−70.73 ± 4.35	170.14 ± 5.08	1.97 ± 1.94	−114.40 ± 14.63
9	−77.46 ± 4.63			−120.40 ± 15.61

The high-resolution structure of *N*spe$_9$ allows for a detailed analysis of the conformational properties of peptoids. Both *cis* and *trans* conformations for the ω torsion angle (corresponding to the peptoid bond) are populated to equal extents (Table 2). The peptoid backbone conforms to the "allowed" regions of the Ramachandran plot for polypeptides. Virtually all ϕ,ψ pairs map to the β-strand region of polypeptides and are strikingly similar to those found in polyproline type I and type II helices (Table 2). Residue **4** is the sole exception, with a positive ϕ value, which maps to the epsilon region of the Ramachandran plot corresponding to turn-like conformations. All *N*spe$_9$ residues populate the same χ^1 rotamer with a torsion angle of about −110°. In this conformation, the side chain methyl and aromatic groups are symmetrically disposed on either side of the plane of the peptoid bond, directed away from the carbonyl oxygen of the preceding residue to avoid steric clashes. The rotamer also precludes clashes between the bulky aromatic group and the carbonyl oxygen of the same residue, irrespective of the conformation around the peptoid bond and the backbone ϕ,ψ values, which are mostly centered around ±70 and 180°, respectively, in the threaded loop conformation

(27) The atomic coordinates for the 20 best structures determined by NMR are available from the authors upon request.

(Table 2). These are in line with predictions via semi-empirical quantum mechanical calculations made previously for model peptoids.[15]

Role of Hydrogen Bonding Interactions on Loop Stability. The shielding of the peptoid backbone from acetonitrile, a solvent devoid of hydrogen bonding potential, coupled with the involvement of key backbone atoms in hydrogen bonding interactions suggested that the threaded loop conformation might be amenable to denaturation via competing hydrogen bonding interactions in other solvents. To test this hypothesis, we recorded a series of CD spectra of *N*spe$_9$ in a variety of solvents with hydrogen bonding potential. In solvents, such as neat TFE, methanol, and TFE/water mixtures, *N*spe$_9$ spectra were characterized by a conspicuous absence of the unique banding pattern detected in acetonitrile (Figure 5A). Consistent with these observations, the *N*spe$_9$ CD spectra recorded in acetonitrile/methanol mixtures underwent dramatic changes in the presence of increasing amounts of methanol, characterized by a reduction in the intensity of the broad minimum at 203 nm accompanied by the appearance of a positive band at 192 nm and negative bands at 202 and 220 nm (Figure 5B). The transition is relatively sharp with the spectral features for the helical conformation readily discernible in 75% acetonitrile/25% methanol, while the threaded loop conformation is completely lost in 50% acetonitrile/50% methanol mixtures.

The involvement of the protonated N-terminus in hydrogen bonding interactions in the threaded loop structure suggested that the conformation would be sensitive to basic pH. To test this idea, a series of CD spectra of *N*spe$_9$ in acetonitrile in the presence of increasing amounts of triethylamine, an organic base, were recorded. The CD spectra exhibited significant changes, mirroring those of the experiments conducted with acetonitrile/methanol solvent mixtures. To evaluate the role of the capping amide group at the C-terminus, an *N*spe$_9$ variant (designated *N*spe$_9$-COOH) lacking the C-terminal NH_2 group was synthesized. The CD spectrum of this variant was almost identical to that of *N*spe$_9$ (Figure 5C), implying that the carboxyl group at the C-terminus was protonated, mimicking the role of the C-terminal capping amide of *N*spe$_9$. The protonated state of the carboxyl group was confirmed by the detection of a downfield resonance (~12 ppm) in the ^{1}H NMR spectrum. Titrations with increasing amounts of triethylamine produced the same trends observed for *N*spe$_9$, including loss of the unique banding pattern characteristic of the threaded loop conformation with a concomitant gain in the spectral features characteristic of the helical conformation (Figure 5C).

Influence of Side Chain Type on the Loop Conformation. To evaluate the role of bulky, aromatic residues toward the stability of the threaded loop structure, *N*spe$_9$ analogues *N*sch$_9$ and *N*ssb$_9$ with side chains of equivalent or reduced bulkiness were prepared and characterized by NMR. Portions of the ^{1}H−^{13}C HSQC spectra of *N*sch$_9$ and *N*ssb$_9$ resembled that of *N*spe$_9$, including the presence of a cluster of four $H^{\alpha 2}$−$C^{\alpha 2}$ correlations with chemical shifts characteristic of a *cis* conformation and another cluster of four with chemical shifts indicative of a *trans* conformation (Supporting Information Figure S4). Interestingly, in the *N*ssb$_9$ spectrum, one of the *cis* peaks and one of the *trans* peaks were much broader than the others, while in the *N*sch$_9$ spectrum, the four *trans* peaks exhibited similar line widths while one of the *cis* peaks was much broader than others.

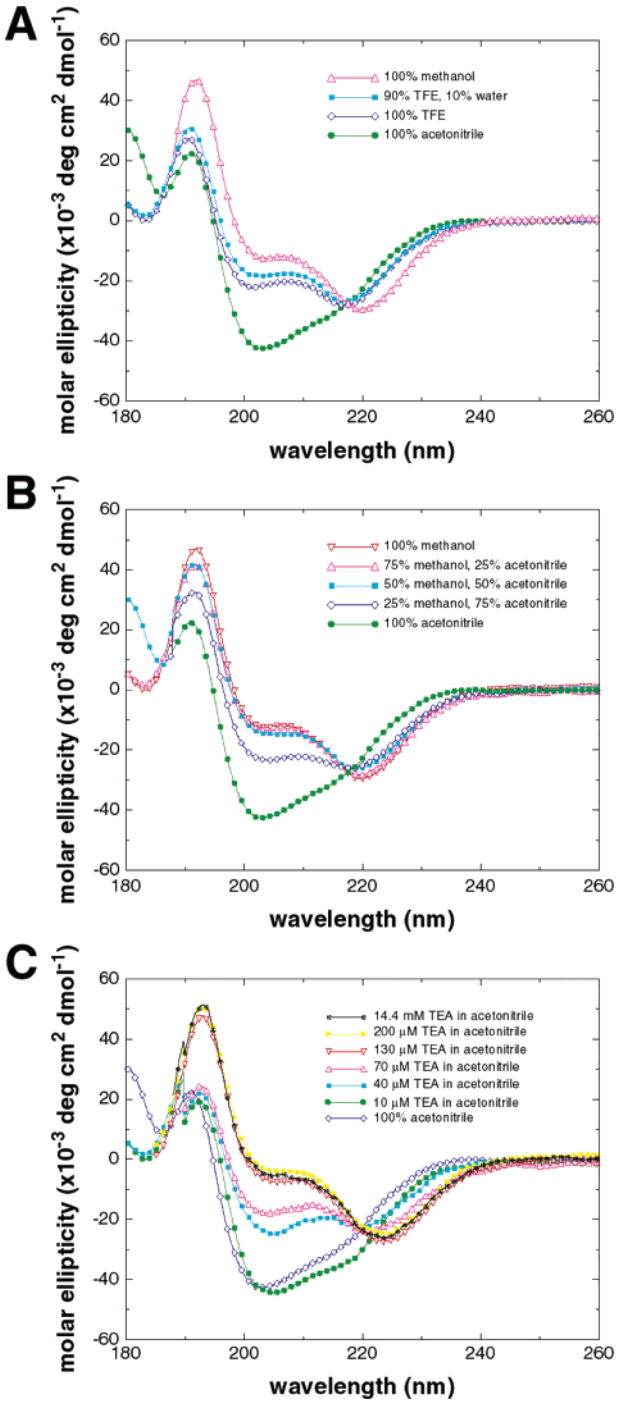

Figure 5. Solvent and pH-induced denaturation of the *N*spe$_9$ threaded loop structure. (A) CD spectra of *N*spe$_9$ recorded in neat acetonitrile, methanol, TFE, and 10% (v/v) TFE in H_2O at 25 °C. Peptoid concentrations were ~60 μM. (B) CD spectra of *N*spe$_9$ in acetonitrile/methanol (% v/v) mixtures ranging from neat acetonitrile to neat methanol in 25% increments recorded at the same temperature. (C) CD spectra of *N*spe$_9$-COOH in acetonitrile recorded as a function of increasing concentrations of triethylamine at 25 °C. Peptoid concentrations were ~60 μM. Notice the lack of changes in the CD spectra at TEA concentrations at or above 130 μM.

Residue **1** of *N*sch$_9$ exhibited two $H^{\alpha 2}$−$C^{\alpha 2}$ correlations of similar intensity, indicating that the N-terminus was in slow exchange on the NMR chemical shift time scale between two distinct conformational states. Collectively, the NMR data suggest that *N*sch$_9$ and *N*ssb$_9$ shared a similar overall structure with *N*spe$_9$, but were more dynamic, perhaps indicative of

reduced stability. The *N*sch$_9$, *N*ssb$_9$, and *N*spe$_9$ oligomers thus define a structurally related peptoid family similar to those found in proteins.

Conclusions

The results described herein demonstrate that peptoids, like proteins, are capable of forming stable, three-dimensional structures. Furthermore, like their natural counterparts, peptoids appear to be endowed with conformational diversity that goes far beyond simple variations of the polyproline type I helical conformation. The factors governing stability of the threaded loop structure include intramolecular hydrogen bonding interactions, bulky side chains that ensure restricted conformational sampling, and indispensable roles for solvent and pH in promoting intramolecular interactions. These factors are similar to those that determine protein structure, although the influence of solvent on the threaded loop conformation is somewhat different from that of water. This distinction notwithstanding, this unique peptoid conformation could be used to test polymer folding algorithms.

Although the current work establishes that nonamer peptoids with bulky side chains could form independently folded structural units, how might this property be gainfully utilized for functional elaboration? We note that the threaded loop conformation could itself be used as a building block to engineer more complex scaffolds, although stability constraints imposed on the N- and C-termini would necessitate covalent linkages involving the main chain C$^\alpha$ carbon. To engineer novel functions, one can seek inspiration from biological macromolecules. Protein active sites are typically characterized by residues from distant parts of the polypeptide chain in close proximity. The side chains of residues **2**, **4**, **6**, and **8** of *N*spe$_9$ define a contiguous surface in the threaded loop structure and thus represent ideal candidates for functional elaboration, including as catalysts for organic reactions or as binding sites for capturing ions or small molecules. Since the structure is susceptible to denaturation by solvents with hydrogen bonding potential and basic pH, this property could be exploited to regulate function. In conclusion, our results establish the possibility of designing molecules with well-defined, three-dimensional structures in nonaqueous environment. This in turn affords opportunities for engineering functions that might otherwise be outside the scope of biopolymers.

Acknowledgment. We wish to thank Barney Yoo for the synthesis of *N*spe$_9$-COOH. This work was supported by a career development award to I.R., from a SPORE grant in Prostate Cancer from NCI (CA90386), and by funds from the NSF and NIH to A.E.B. I.R. is a Scholar of the Leukemia and Lymphoma Society. J.A.P. was supported by an NIH Molecular Biophysics training grant. We gratefully acknowledge the Robert Lurie Comprehensive Cancer Center for supporting structural biology research at Northwestern.

Supporting Information Available: The Experimental Section, the full citation for ref 7, supplementary figures, including the CD spectra of *N*rpe$_9$ and *N*spe$_9$, illustration of the strategy used for peptoid resonance assignment, expanded contour plots of a ROESY spectrum of *N*spe$_9$, expanded plots of ^{1}H$-^{13}$C HSQC spectra of *N*spe$_9$, *N*sch$_9$, and *N*ssb$_9$. This material is available free of charge via the Internet at http://pubs.acs.org.

JA0574318